

# Haptic Control for Steer-by-Wire Systems

N. Bajcinca

Institute of Robotics and Mechatronics  
DLR, Oberpfaffenhofen, Germany  
email: [naim.bajcinca@dlr.de](mailto:naim.bajcinca@dlr.de)

R. Cortesão

Institute of Systems and Robotics  
ISR, Coimbra, Portugal  
email: [cortesao@isr.uc.pt](mailto:cortesao@isr.uc.pt)

M. Hauschild

Institute of Robotics and Mechatronics  
DLR, Oberpfaffenhofen, Germany  
email: [markus.hauschild@dlr.de](mailto:markus.hauschild@dlr.de)

J. Bals

Institute of Robotics and Mechatronics  
DLR, Oberpfaffenhofen, Germany  
email: [johann.bals@dlr.de](mailto:johann.bals@dlr.de)

G. Hirzinger

Institute of Robotics and Mechatronics  
DLR, Oberpfaffenhofen, Germany  
email: [gerd.hirzinger@dlr.de](mailto:gerd.hirzinger@dlr.de)

**Abstract**— A force-feedback actuation loop for a steer-by-wire vehicle is developed. It is shown that the performance of this loop can be essentially improved by the introduction of a torque sensor. Model reference based control algorithms based on disturbance observer (DOB) and active observers (AOB) are applied to enhance the robustness vs. non-modelled dynamics and uncertain driver impedance.

## I. INTRODUCTION

Steer-by-wire steering technology replaces the mechanical interface (steering column) between the driver and vehicle by a highly complex mechatronical system, consisting of computing units, sensors and actuators. A steer-by-wire system is basically a *master-slave* system: the driver corresponds to the *operator*, the vehicle to the *environment*, the force-feedback actuator to the *master* and the front-wheel actuator to the *slave*. From the control point of view, a steer-by-wire system includes a force feedback inner-loop on the master side and a position or force inner-loop on the slave side, which are coupled by a suitable outer-loop controller to provide a desired steering feeling to the driver and desired steering response to the vehicle. This paper focuses on the force-feedback actuation loop.

Most approaches on today's design stage of steer-by-wire vehicles include feed-forward open-loop torque control, that is, due to cost matter torque sensors are avoided. While high-performance direct-drives may offer satisfactory behavior, the efficiency of such loops decreases essentially due to the absence of torque amplification by gearing. However, in a geared force-feedback actuation, the performance of feed-forward control is limited because of the lack of friction compensation, unmodeled dynamics and disturbance rejection. While these tasks may be set to the outer-loop controller, solving them in a closed inner-loop would burden outer-loop controller and would provide more robustness to the performance of the overall steer-by-wire system. This paper follows the design of force-feedback actuation loop based on the latter strategy.

The essential components of the used force-feedback actuator are a servo-motor, a harmonic-drive gear and a torque sensor. Apart from ripple compensations on the output torque of the Harmonic-Drive gear, the main challenge is to provide robustness with respect to uncertainties of the driver stiffness, which may change within a large

interval. In order to cope with modeling errors, disturbances and uncertainties, the model-reference (adaptive) control approach is investigated, that is, instead of fitting the physical model into a mathematical one, the opposite is tempted, the physical model is forced to fit into a mathematical description, by introducing correction signals at the input. Therefore, the observer-based algorithms: Disturbance Observer (DOB), [5] and Active Observer (AOB), [2] are used.

The paper is organized as follows. Section II includes system modeling items, discussion of force-feedback control in the context of the steer-by-wire and details about the components of the the steer-by-wire test-bed. Section III recalls the basic theory of the disturbance observer and Section IV the basics of the active observer algorithm. In Section V robustness with respect to the driver stiffness and quality of driving feeling are linked with sensitivity function of torque closed-loop. Section VI presents simulation results and finally, Section VII presents experimental results with DOB and AOB.

## II. SYSTEM MODELING

Fig. 1 shows a simplified interaction scheme of the driver and a steer-by-wire vehicle via a force-feedback actuator. Thereby,  $\tau_d$  stands for the forces generated at the muscles of the driver,  $\tau_r$  is the command signal generated by the steer-by-wire controller, i.e. the reaction torque which the driver should feel,  $\delta_h$  is the steering angle and  $\delta_s$  stands for the lateral position of the steering link (i.e. rack position). The front-wheel actuation, vehicle dynamics reaction (impedance) and the actuation coupling control (steer-by-wire controller) are included within the *Steer-by-Wire Vehicle* block. The *Driver Impedance* block represents the passive bio-mechanical impedance of the driver arm. This paper focuses on the block *Force Feedback Actuation*.

Fig. 2 gives a simple description of the torque balance on the steering-wheel with driver-in-the-loop ( $Z_d \neq 0$ ). Thereby,  $\tau_f$  is the output written by the torque-feedback loop in response to the command signal  $\tau_r$ , and  $\tau'$  is the net torque felt by the driver. This loop will be revisited in Section V, where the robustness of the loop with respect to driver impedance uncertainties is discussed.

Basically in a steer-by-wire system (and in general in

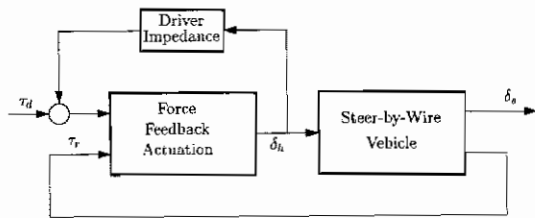


Fig. 1. Force-feedback in a steer-by-wire vehicle.

force-feedback control) two approaches are possible. In the so-called *open-loop* force control, the torques applied on the driver are not sensed, i.e. a feed-forward control scheme is used. Its disadvantage is that in reality torque differs from the computed one, owing to several factors such as system noise, friction and inertia in the interface mechanism. To compensate for the above effects and improve control accuracy and performance, the interface needs to incorporate a torque sensor. This is usually called *closed-loop* force control in force-feedback literature [1].

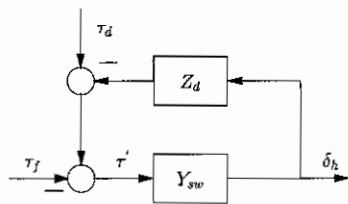


Fig. 2. The driver impedance loop.

### A. The Steer-by-Wire Setup

This section provides a description of steer-by-wire force-feedback actuator. In the sequel, the hardware components of the actuator are presented. This is followed by a discussion on its dynamics and bio-mechanical driver impedance.

#### A.1 Harmonic-Drive Gear

The main component in the the force-feedback actuator, Fig. 3, is Harmonic-Drive FHA Series Hollow-Shaft Actuator. It consists of a sine-commutated AC servo motor with built-in incremental encoder and a Harmonic-Drive gear.

The steering wheel is mounted directly on the gear output shaft. Due to the high single stage gear transmission of  $N = 50$ , a compact unit is designed, that provides an output torque of up to approximately  $50 \text{ Nm}$ . Advantages of this actuation are the virtually zero backlash, reversibility of the Harmonic-Drive gears and back-driving in an emergency situation. However, various effects such as friction, the torque ripple typical for Harmonic-Drive gears and the motor moment of inertia need to be compensated to provide a smooth steering feeling, comparable to the feeling of a mechanical steering mechanism of today's vehicles.

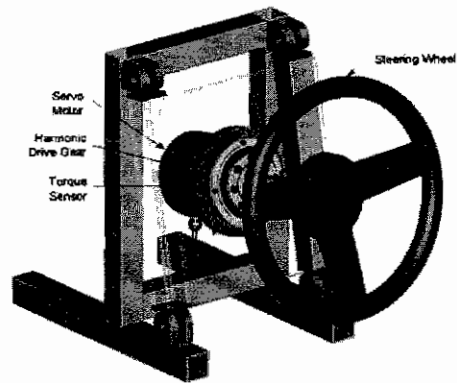


Fig. 3. Force-feedback actuator.

#### A.2 Torque Sensor

The function of the torque sensor is based on strain gauges. This operating principle implies that an additional elasticity is introduced into the mechanical system which accounts for approximately one third of the entire gear elasticity. The use of two independent measurement bridges provides redundancy and also allows the compensation of temperature changes and other disturbances.

#### B. Actuator Modelling

Fig. 4 depicts a simplified schematic model of the FHA actuator. It includes the moments of inertia of rotor and housing and the elasticities of torque sensor and Harmonic-Drive gear, modelled as spring-damper systems. Thereby, it can be shown that the non-minimum phase zero in the model is caused by the elasticity of the strain gauges. However, this zero is not dynamically critical, because of the high sensor stiffness.

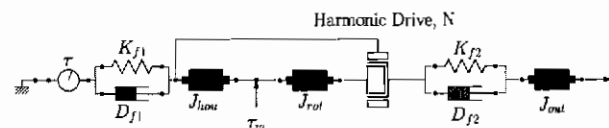


Fig. 4. Physical model of the force-feedback actuator.

- $N$ : Gear transmission ratio
- $J_{out}$ : Gear output inertia
- $D_{f1}$ : Sensor damping
- $K_{f1}$ : Sensor stiffness
- $D_{f2}$ : Gear damping
- $K_{f2}$ : Gear stiffness
- $J_{hou}$ : Motor housing inertia
- $J_{rot}$ : Rotor inertia
- Input: Torque on the rotor shaft
- Output: Reflected (reaction) torque on steering wheel

The essential torque components measured by the sensor are included in the following approximate equation,

$$\tau = P_l \tau_m + \tau_f + \tau_{nl}, \quad (1)$$

whereby,

- $\tau$ : Measured torque
- $P_l$ : Linear torque transfer function
- $\tau_m$ : Motor torque
- $\tau_{nl}$ : Non-linear friction components

Model-based control approaches require good models for all these components, which is a rather difficult task. In addition, the driver impedance is  $Z_d$  is highly uncertain, since the driver may hold the steering wheel tight (high  $Z_d$ ) or let it free ( $Z_d = 0$ ). To overcome these problems, in this paper a model reference control approach will be used, that is, the components which are hard to model or are uncertain are considered simply as disturbances. Thus, the open-loop is described by the approximate simple equation,

$$\tau = P_l \tau_m + \text{disturbances}. \quad (2)$$

Notice that the component *disturbances* in the latter equation is assumed to include also the torque ripple, which is periodic with its fundamental component corresponding to twice the frequency of the motor shaft speed.

### C. Bio-mechanical human arm impedance

The impedance of the human arm describes the force/velocity relationship  $F = Z(v)$ , whereby  $Z(v)$  is some nonlinear function, [4]. The exact modelling of human arm is yet a complex problem; nonlinear modelling does not really provide essentially better results than the linear one. However, the muscle actuator of the driver arm may be roughly modelled by a linear equation as follows,

$$\Delta x = g_{m\alpha} \Delta f_\alpha + g_{mf} f_m, \quad (3)$$

whereby

- $x$ , Internal muscle length
- $\Delta f_\alpha$ , Nerve excitation of the  $\alpha$ -neuron
- $f_m$ , Force acting on the muscle
- $g_{m\alpha}$ , Feedforward control of muscle length
- $g_{mf}$ , Driving point admittance.

The transfer functions in this equation depend on muscle stiffness, muscle damping and the combined mass of the limb and interface element (i.e. steering wheel). The feedforward transfer function affects the muscle length through changes of afferent neural activation  $\Delta f_\alpha$  and the adaption of arm impedance and control of arm position is based on feedback of neural activation. It has been shown that the impedance adaption feedback loop is a low bandwidth one, 1.7 Hz. As a common modelling approach of the driving point impedance of the human arm has been accepted the variable spring-like behavior, whereby its stiffness is modified by neural feedback. Measurement suggest, [3], minimal incremental elbow stiffness of 2 Nm/rad and maximal of 400 Nm/rad. On the other hand, the damping was estimated to be around 5.5 N s/m, thus indicating that the human arm is lightly damped.

### III. DOB BASED CONTROL

The disturbance-observer control method uses the inverse model approach for the design of a two degree of freedom control architecture [5], by providing both, feedforward and feedback control. Its scheme is shown in Fig. 5.

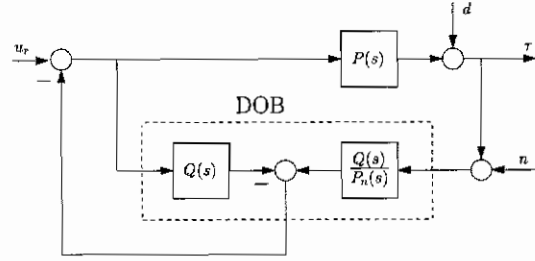


Fig. 5. Disturbance observer scheme for force control.

It can be shown that sensitivity  $S(j\omega)$  and complementary sensitivity  $T(j\omega)$  functions of this structure are as follows,

$$S := \frac{\tau}{d} = \frac{1}{1+L} = \frac{P_n(1-Q)}{P_n + (P-P_n)Q} \quad (4)$$

$$T := \frac{\tau}{n} = \frac{L}{1+L} = \frac{QP}{P_n + (P-P_n)Q}, \quad (5)$$

whereby the open-loop transfer function,  $L$ , is easily shown to be,

$$L = \frac{PQ}{P_n(1-Q)}. \quad (6)$$

Notice that the DOB structure introduces two functions,  $P_n(s)$ , which is called *nominal* (or *target*) plant and a filter  $Q(s)$ . The basic idea of the DOB approach is to force the behavior of the overall system in the operating frequency range be as that of the nominal plant  $P_n$ . Indeed, the transfer function from  $u_r$  to  $\tau$  in the DOB scheme is,

$$\frac{\tau}{u_r} = \frac{PP_n}{P_n + (P-P_n)Q}, \quad (7)$$

which for the frequencies where  $|Q(j\omega)| \approx 1$ , tends to  $P_n$ . On the other side, notice that because of  $S(j\omega) \rightarrow 0$ , the system response on disturbances  $d$  is minimized at these frequencies, while the response is highly sensitive on measurement noise  $n$ ,  $T(j\omega) \rightarrow 1$ . Fortunately in most applications the disturbance  $d$  is low frequent, while measurement noises are high-frequent. Therefore, for a given application the design task of the filter  $Q$  is to shape it in such a way that  $|Q(j\omega)| \approx 1$  in the frequency range of interest (usually low frequencies), and to let it tend to zero  $|Q(j\omega)| \rightarrow 0$  for higher frequencies for noise attenuation.

### IV. AOB BASED CONTROL

A linear system represented in state space by

$$\begin{cases} x_{r,k} = \Phi_r x_{r,k-1} + \Gamma_r u_{k-1} \\ y_k = C_r x_{r,k}, \end{cases} \quad (8)$$

can be controlled through state feedback (e.g. optimal control, adaptive control, deadbeat control and "pure" pole placement control). In practice, the main problem of this approach is that (8) does not represent exactly the real

system. In fact, unmodeled terms including noise, higher order dynamics, parameter mismatches, couplings and unknown disturbances are not addressed in the control design. Therefore, it is necessary to develop a control structure that can deal with them, so that the overall system may have the desired behavior. The AOB state space control design satisfies these requirements.

The main goal of the AOB is to fit a physical system (i.e. its input/output behavior) into a linear mathematical model, rather than to fit a mathematical model into a physical system. To accomplish this goal, a description of the system (closed loop and open loop) is necessary. A special Kalman Filter (KF) has to be designed. The motivation for this special KF is based on:

1. A desired closed loop system for the state estimation.
2. An extra equation to estimate an equivalent disturbance referred to the system input. An active state  $p_k$  (extra-state) is introduced to compensate unmodeled terms, providing a feedforward compensation action.
3. The stochastic design of the Kalman matrices  $Q$  and  $R$  for the AOB context. Model reference adaptive control appears if  $Q_{x_{r,k}}$  is much smaller than  $Q_{p_k}$ . In this case, the estimation for the system state follows the reference model. Everything that does not fit in the  $x_{r,k}$  model goes to  $p_k$ . In the sequel, the first-order AOB algorithm<sup>1</sup> will be described.

Controlling the system of (8) through state feedback from an observer and inserting  $p_k$  in the loop, the overall system can be described by

$$\begin{bmatrix} x_{r,k} \\ p_k \end{bmatrix} = \begin{bmatrix} \Phi_r & \Gamma_r \\ 0 & 1 \end{bmatrix} \begin{bmatrix} x_{r,k-1} \\ p_{k-1} \end{bmatrix} + \begin{bmatrix} \Gamma_r \\ 0 \end{bmatrix} u_{k-1} + d_k \quad (9)$$

and

$$y_k = C_a \begin{bmatrix} x_{r,k-1} & p_{k-1} \end{bmatrix}^T + n_k, \quad (10)$$

where

$$u_{k-1} = r_{k-1} - \begin{bmatrix} L_r & 1 \end{bmatrix} \begin{bmatrix} \hat{x}_{r,k-1} \\ \hat{p}_{k-1} \end{bmatrix}. \quad (11)$$

The stochastic inputs  $d_k$  and  $n_k$  represent respectively model and measure uncertainties. The state estimate of (9) is based on the desired closed loop (i.e.  $\hat{p}_k = p_k$  and  $\hat{x}_{r,k} = x_{r,k}$ ). It is

$$\begin{bmatrix} \hat{x}_{r,k} \\ \hat{p}_k \end{bmatrix} = \begin{bmatrix} \Phi_r - \Gamma_r L_r & 0 \\ 0 & 1 \end{bmatrix} \begin{bmatrix} \hat{x}_{r,k-1} \\ \hat{p}_{k-1} \end{bmatrix} + \begin{bmatrix} \Gamma_r \\ 0 \end{bmatrix} r_{k-1} + K_k (y_k - \hat{y}_k), \quad (12)$$

with

$$\hat{y}_k = C_a \left( \begin{bmatrix} \Phi_r - \Gamma_r L_r & 0 \\ 0 & 1 \end{bmatrix} \begin{bmatrix} \hat{x}_{r,k-1} \\ \hat{p}_{k-1} \end{bmatrix} + \begin{bmatrix} \Gamma_r \\ 0 \end{bmatrix} r_{k-1} \right) \quad (13)$$

<sup>1</sup>The general AOB algorithm uses  $N$  extra states to describe  $p_k$  [2].

and

$$C_a = \begin{bmatrix} C_r & 0 \end{bmatrix}. \quad (14)$$

The Kalman gain  $K_k$  reflects the uncertainty associated to each state based on model and measure uncertainties. It is computed from

$$K_k = P_{1k} C_a^T [C_a P_{1k} C_a^T + R_k]^{-1}, \quad (15)$$

with

$$P_{1k} = \Phi_n P_{k-1} \Phi_n^T + Q_k \quad (16)$$

and

$$P_k = P_{1k} - K_k C_a P_{1k}. \quad (17)$$

$\Phi_n$  is the augmented open loop matrix,

$$\Phi_n = \begin{bmatrix} \Phi_r & \Gamma_r \\ 0 & 1 \end{bmatrix}. \quad (18)$$

$Q_k$  is the system noise matrix and represents model uncertainty. It is given by

$$Q_k = \begin{bmatrix} Q_{x_{r,k}} & 0 \\ 0 & Q_{p_k} \end{bmatrix}. \quad (19)$$

The measurement noise matrix  $R_k$  represents measure uncertainty.  $P_k$  is the mean square error matrix. Its initial value should reflect at least the uncertainty in the state estimation. It should not be lower than the initial matrix  $Q_k$ .

## V. ROBUSTNESS AND TUNING OF THE DRIVING FEELING

The loop in Fig. 6 describes the interaction of the driver with the force-feedback actuator. Thereby, it is assumed that the commanded force on the torque control-loop is zero and the disturbances are neglected. As already noted,  $\tau_d$  represents the force generated in the muscles of the driver,  $\delta_h$  the steering angle and  $S$  stands for the sensitivity function of the torque closed-loop. There are two main reasons for the investigation of this loop: (a) robustness with respect to the driving point impedance  $Z_d$ , and (b) correction (tuning) of the transfer function  $\tau_d \mapsto \delta_h$ , which is indicative for the driving feeling. These set additional specifications on the design of the torque closed-loop.

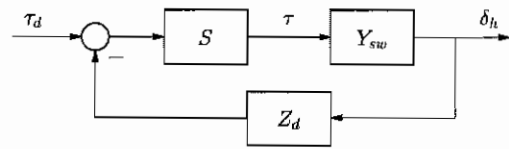


Fig. 6. For the provision of a better feeling and robustness,  $S$  needs to be shaped accordingly.

It is straightforward to show that robustness criterion with respect to  $Z_d$  is satisfied if

$$|S(j\omega)Y_{sw}(j\omega)Z_d(j\omega)| \ll 1. \quad (20)$$

While DOB algorithm already satisfies this condition qualitatively (remember  $S(j\omega) \rightarrow 0$ ), notice that the above equation define the upper bound of the sensitivity function.

Eq. (21) yields the approximate equation, which describes the driving feeling,

$$\delta_h \approx S(j\omega)Y_{sw}(j\omega)\tau_d. \quad (21)$$

Two statements yield from this equation: (1) specification  $S(j\omega) = 0$  in the driving (i.e. low) frequency range does not make sense, since this would put the driver out of loop, and (2) tuning of the driving feeling may be directly done via shaping of the sensitivity function  $S(j\omega)$ .

Experimental results on the setup have shown that transfer function  $\tau_d \rightarrow \delta_h$  may need additional damping for the improvement of the driving feeling. A solution proposed in this paper is shown in Fig. 7, whereby an additional controller is added in cascade with DOB structure.

The sensitivity function of the new structure is now,

$$S = \frac{P_n(1-Q)}{P_n(1-Q) + P(Q + P_n C)}, \quad (22)$$

and a simple controller which damps the driving feeling is a PD controller, i.e.  $C(s) = P + Ds$ .

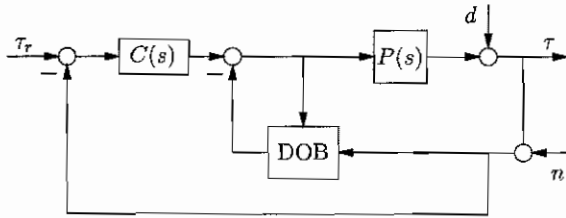


Fig. 7. Adding a PD controller may improve the driving feeling.

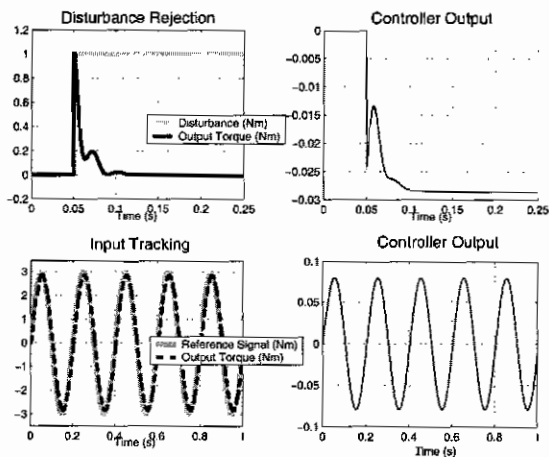


Fig. 8. Simulation results with DOB control for  $Z_d \rightarrow \infty$ .

## VI. SIMULATION RESULTS

Simulation results for the both control structures: DOB (Fig. 8) and AOB (Fig. 9) are collected in this section. Since driver impedance is difficult to model, just the well-defined situation with the fixed steering-wheel ( $\delta_h = 0$ ) is considered. Two scenarios have been investigated: (a) output disturbance rejection and (b) input tracking. The performance is shown on the left side, while the respective controller output (DOB), i.e. active state response (AOB) are shown on the right side. Notice that the performance of the both structures is comparable.

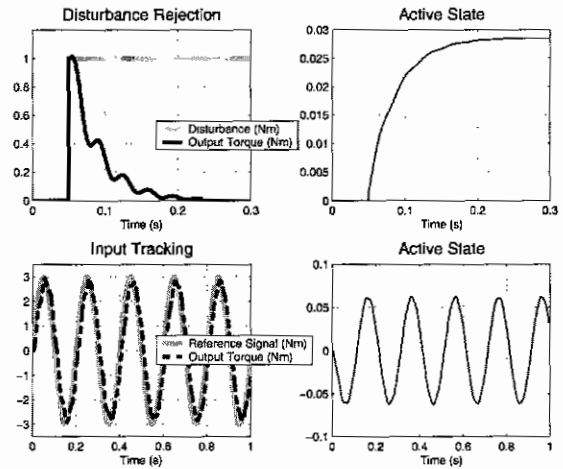


Fig. 9. Simulation results with AOB control for  $Z_d \rightarrow \infty$ .

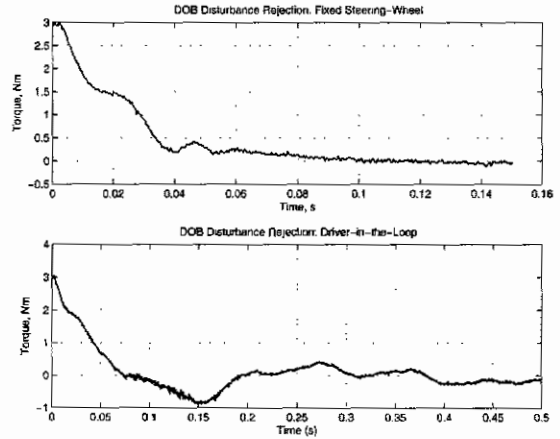


Fig. 10. Disturbance rejection with DOB control.

## VII. EXPERIMENTAL RESULTS

This section shows the experimental results with DOB and AOB algorithm. DOB controller is designed using a fourth order target plant  $P_n$  and a Butterworth  $Q$ -filter of fourth-order, while the AOB algorithms of the first order have been used.

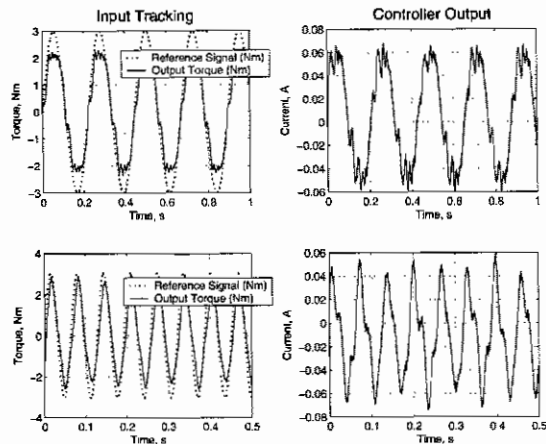


Fig. 11. Torque tracking responses of the DOB loop for  $Z_d \rightarrow \infty$ .

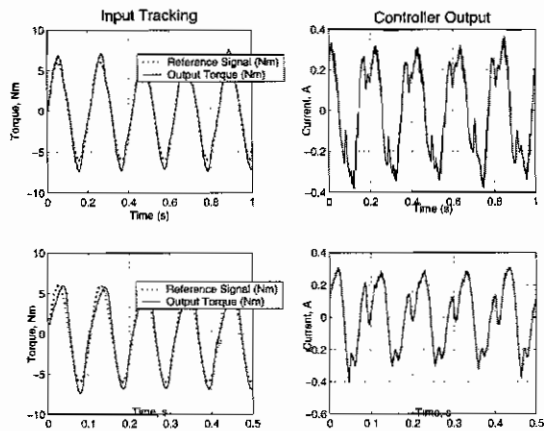


Fig. 12. Torque tracking responses of the DOB with driver-in-the-loop.

## VIII. CONCLUSIONS

A high bandwidth force actuation system for steer-by-wire vehicles is presented in this paper. Rather than open-loop force control, the closed-loop force control strategy is followed by installing a torque sensor in the force-feedback actuator. The model reference based control approach is used, that is, instead of putting effort in modelling the processes, which are difficult to model (e.g. torque ripples) or are highly uncertain (driver impedance), observer-based algorithms are used to cancel the non-modelled physical

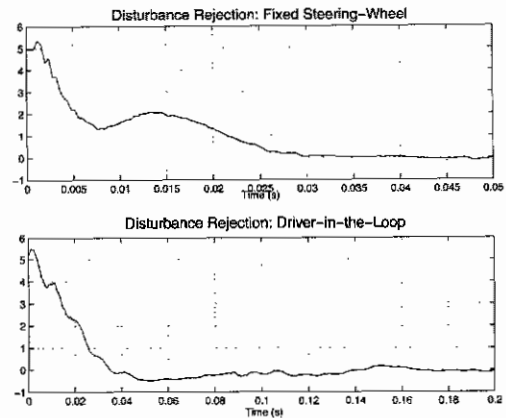


Fig. 13. Disturbance rejection of AOB.

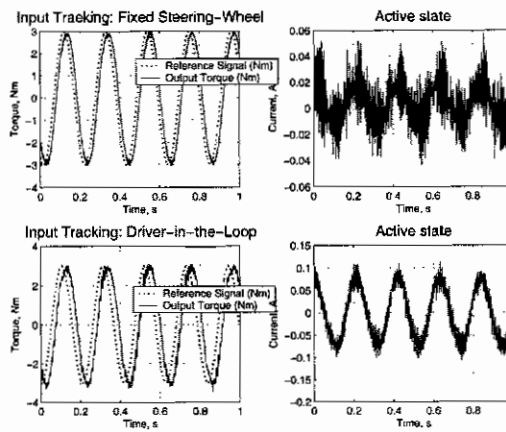


Fig. 14. Torque tracking of AOB loop.

dynamics. Thereby, the disturbance-observer (DOB) and active-observer (AOB) control has been applied. While a certain reluctance in applying the harmonic-drive gearing technology because of the torque ripples is at the present noticeable, this paper shows that at the expense of an additional torque sensor, high-bandwidth robust and smooth torque control is feasible. It is shown that by shaping sensitivity function in the driving frequency bandwidth the robustness and driving feeling may be tuned. Simulation and experimental results validate the proposed approach.

## REFERENCES

- [1] Grigore C. Burdea. *Force and Touch Feedback for Virtual Reality*. John Wiley, 1996.
- [2] R. Cortesão. *Kalman Techniques for Intelligent Control Systems: Theory and Robotic Experiments*. PhD thesis, University of Coimbra, 2003.
- [3] N. Hogan. Controlling impedance at the man/machine interface. *Proc. of the IEEE Int. Conference on Robotics and Automation*, 1989.
- [4] R. Koeppel. *Robot Compliant Motion based on Human Skill*. PhD thesis, Swiss Federal Institute of Technology, 2001.
- [5] K. Ohnishi. A new servo method in mechatronics. *Trans. Japanese Society of Electrical Engineering*, 107-D:83–86, 1987.